Rubber to liquid transition in amorphous polymer thin films

Adrien Delanoe,[1] David Siniscalco, [1,2] Viktoriia Drebezghova, [3] Philippe Leclère,[4] Guillaume Vignaud [5] and Nicolas Delorme [1,]*

1 Institut des Molécules et Matériaux du Mans (IMMM) – UMR CNRS 6283 – Le Mans Université, Avenue Olivier Messiaen, 72000 Le Mans, France

2 Institut Supérieur des Matériaux et Mécaniques Avancées du Mans (ISMANS Groupe CESI), 44 avenue Frédéric Auguste Bartholdi, 72000 Le Mans, France

3 Université d'Orléans, CNRS, Interfaces Confinement Matériaux et Nanostructures, 3 Avenue de la Recherche Scientifique, 45071 Orleans, France

4 Laboratory for Physics of Nanomaterials and Energy (LPNE), Research Institute for Materials Science and Engineering, University of Mons (UMONS), 20 Place du Parc, B 7000, Mons, Belgium

5 Laboratoire d'Ingénierie des Matériaux de Bretagne (LIMATB)– Université de Bretagne Sud, Rue Saint Maudé, 56321 Lorient, France

KEYWORDS : Glass transition temperature ; polymer ; thin film ; confinement; Atomic Force Microscopy

ABSTRACT

The characterization of the thermomechanical properties of thin polymer films is of critical importance for a wide range of applications, including microelectronics, functional coatings, and biomedical devices. However, reliable measurements at the nanoscale remain challenging due to

confinement effects, substrate influence, and the limitations of conventional experimental techniques. In this work, we introduce a novel experimental approach to probe the thermomechanical behavior of thin polymer films based on pull-off force measurements performed using Atomic Force Microscopy (AFM). The evolution of adhesion forces with temperature provides direct insight into thermal transitions and mechanical softening phenomena occurring within confined polymer layers. The proposed method offers high spatial resolution and sensitivity, enabling the investigation of films with thicknesses down to a few tens of nanometers. In addition to the measurement of the glass transition temperature (Tg), a characteristic temperature (Tmax) is identified, at which the maximum pull-off value is observed. The strong link between Tg and Tmax is demonstrated by the effect of chain length and confinement. ~~Our results indicate that Tmax corresponds to the beginning of the rubber-to-liquid transition, which ends at the crossover temperature (Tc) predicted by the MCT theory.~~

Introduction

Temperature strongly affects polymer properties because chain mobility, free volume, and phase state all change with temperature. For amorphous polymers, the glass transition temperature is used as a reference to describe the thermomechanical properties. The glass transition temperature (Tg) is commonly described as the transition from a low-temperature glassy (brittle) state to a rubbery and deformable state. Despite its importance, the glass transition remains a long-standing unsolved problem in materials science because it involves complex interplay between intramolecular and intermolecular cooperativity.[1] In addition to Tg, amorphous polymers exhibit several secondary relaxation processes. Below Tg, transitions are associated with movements involving a side group of the chain, a few monomers, or even the entire polymer chain.[2,3]

The existence of transitions above Tg has been confirmed by numerous experimental approaches, including dynamic dielectric spectroscopy,[4,5] energy dissipation analysis,[6] low-frequency anelastic spectroscopy,[7] and nuclear magnetic resonance.[8] In 1963, Boyer [9] proposed the existence of a transition temperature at T>Tg, named T_{ll} corresponding to a thermodynamic liquid-liquid transition. In subsequent studies,[10,11] they found that this transition was linked to Tg and located approximately at 1,2×Tg, concluding that they were both governed by the same type of molecular motion but in different ranges. The existence of T_{ll} was quickly criticized because the transition was experimentally difficult to detect[12] and at this time no established model was able to predict a relaxation above Tg.[13] In addition to Boyer's interpretation, different approaches have been proposed for the origin of this transition. Hedvat *et al.* proposed that T_{ll} corresponds to a maximum of energy dissipation and can be associated to a rubber-viscous transition due to a coilling-uncoilloing process.[14] More recent works attribute the transition temperature at 1,2×Tg to a pure dynamic process corresponding to a crossover temperature from solid-like to liquid-like dynamics such as predicted by the mode-coupling theory (MCT).[5,15–17] MCT remains a central theoretical framework to describe the dynamic crossover in glass-forming systems and has been the subject of recent critical assessments clarifying its physical content and limitations.[18] Recent extensions such as generalized mode-coupling theory (GMCT) further support the existence of a dynamical crossover while providing improved descriptions of slow relaxation phenomena in supercooled liquids and polymers.[19]

In addition, numerous experimental and theoretical investigations demonstrate that reducing thickness in polymer films below the bulk regime induces deviations in the glass transition temperature.[20] These effects are commonly attributed to confinement-induced alterations in chain mobility, the presence of interfacial layers with distinct dynamics, and the suppression of

cooperative segmental motions.[21,22] As a consequence, such thickness-dependent effect will have direct implications for the thermal stability, mechanical integrity, and long-term reliability of polymer films in applications ranging from nanoelectronics to barrier coatings.[23] Very few studies have so far addressed the effect of confinement on amorphous polymer film properties above Tg. In this work, a novel experimental approach is introduced to probe the thermomechanical behavior around and above their Tg of thin polymer films based on pull-off force measurements performed using Atomic Force Microscopy (AFM). The evolution of adhesion forces with temperature provides direct insight into thermal transitions and mechanical softening phenomena occurring within confined polymer layers. We aim to verify the presence of characteristic temperatures above the glass transition temperature (Tg) in amorphous polymers and to investigate their relationship with Tg through variations in molecular weight (Mn) and the effects of confinement.

Materials and Methods

Material

Atactic polystyrene (PS) samples with different molecular weights (Mn=20, 136, 783, 996 and 1500 kg/mol) and dispersity <1.1 were purchased from Polymer Source®. Bulk Tg (Figure S1) were measured by Differential Scanning Calorimetry (DSC). Except Mn=20k where Tg=361(2)K, all the samples show a Tg=377(2)K.

Polymer thin-film preparation

Thin films were prepared by spin-coating filtered PS solution in toluene on silicon wafer containing a silica (SiO_2) native layer. The substrates were cleaned by sonication in a (CH_3OH + HCl in 1:1 v/v) solution at room temperature, the silicon wafers were rinsed with deionized water and then treated for 15 minutes in an UV-ozone chamber in order to remove organic contaminants

and improve film stability.[24] Spin-coating conditions were optimized to obtain homogeneous high-quality film with controlled thickness and low surface roughness (Sq<0.4 nm for 5x5µm² surface). Polymer films were then annealed under a vacuum at 160°C for 24 h in order to decrease surface stresses induced by the deposition method. Film thicknesses were measured by ellipsometry after annealing.

Transition temperature measurements of thin films by Atomic Force Microscopy

All AFM measurements were performed on an Agilent 5500 AFM equipped with an environmental chamber and controlled humidity. The instrument was operated with the PicoView software. Temperature control was monitored by a PID controller (Lakeshore) associated to a heat stage allowing heating from T = 20°C to 250°C with an accuracy of 0.1°C. Temperature controller was calibrated before each measurement with three standard fusion point solids (benzophenone (T_f=48°C), azobenzene (T_f=68°C) and acetanilide ($T_f = 114.5°C$)).

Force distance curves were acquired using different Biosphere® B40-FM spherical diamond tips with tip radius of 40(5) nm with spring constant ranging between 1.76 N/m and 3.01 N/m, respectively. Spring constants were calibrated using the direct force method with reference cantilevers. While AFM tip geometry, stiffness, and chemical nature are acknowledged to potentially influence adhesion strength, Figure S2 demonstrates the independence of T_{max} detection with respect to these parameters. Regardless of the AFM tip selected, a maximum load force of 130(10) nN and a loading/unloading rate of 4 µm·s^{-1} were consistently applied.[25] Starting from T=30°C until the ending temperature, forces curves were acquired every 2°C after a stepwise heating (2°C/min) and an equilibration time of 1 min.

~~All the force-distance curves were conducted at 1 Hz in order to work in a quasi-static regime where rate effects are expected to be minimal~~ All these parameters were kept constant for all temperatures, film thicknesses, and molecular weights. ~~Details on the pull-off force measurement method can be found in a previous publication.~~ Pull-off force value was measured from the retraction force distance curve as the difference between the minimum force and the force at a large surface distance. For each temperature, 4 different locations were chosen on which 10 force-distance curves were averaged to give the pull-off force intensities and uncertainties. Data processing and analysis were carried out using the open-source software AtomicJ®.

Ellipsometry Measurements

Spectroscopic ellipsometry measurements were performed using a Horiba UVISEL apparatus equipped with a heating stage. The ellipsometric angles Ψ and Δ were recorded as a function of temperature at a fixed incident angle of 70° over a wavelength range from 275 to 1771 nm. Following the same procedure that for the pull off force measurements, for each temperature, the sample was held for 1 min to ensure thermal equilibration before data acquisition. Measurements were carried out upon heating at a rate of 2 °C/min. Data processing and analysis were performed using the DeltaPsi 2.24 software.[26]

Nano-Dynamic Mechanical Analysis

AFM nano-DMA is a recently developed AFM mode to quantify the viscoelastic properties at the nanoscale. [27] The “measurement process” is similar to force−distance curve measurement, except that when the tip is in contact with the studied sample, the load is maintained and a frequency modulation is applied to the tip. The difference of phase between the dynamic solicitation on and the cantilever deflection, coupled with the force−curves analysis, gives access to local rheological

parameters of the sample, such as storage modulus (E′), loss modulus (E″), and damping factor (tan δ). AFM nano-DMA has two modes. The first is an imaging mode where the frequency modulation is fixed and the tip scans the surface, providing quantitative mapping of viscoelastic properties. The second is a spectroscopic mode where the position of the tip is fixed while a ramp script of discrete frequencies is applied, providing the evolution of rheological properties as a function of those frequencies. All nano-DMA measurements were performed on a Dimension Icon AFM (Bruker Corp.). Temperature control was monitored by a PID controller (Lakeshore) connected to a heat stage inside the AFM device. The probes used are pre-calibrated RTESPA 300-30 cantilevers from Bruker Corp. with a spring constant around 40 $N.m^{-1}$ and a nominal tip radius of 30 nm. All measurements were done in spectroscopic mode with frequencies randomly chosen within the range from 1 to 160 Hz. For each temperature nano-DMA measurements were carried out at six distinct and spatially separated points to account for local variability. The homogeneity in terms of morphology and mechanical properties (adhesion, rigidity modulus, and indentation) of those areas were previously checked by Peak Force Tapping mode. Nanoscope Analysis 3.0 was used to analyze and extract the data.

Temperature dependency of the work of adhesion between the AFM tip and the PS surface

The work of adhesion between the AFM Diamond-like carbon (DLC) tip and the PS surface was calculated using the following the Berthelot rule: $W_0 = 2\sqrt{\gamma_{PS} \times \gamma_{DLC}}$ [28] where γ_{PS} and γ_{DLC} are the surface solid energies of the film and the AFM tip respectively. γ_{PS} was determined using the Neumann method[28] by measuring the glycerol contact angle on a Biolin Attension® goniometer equipped with a controlled and calibrated heating system. γ_{DLC} values were extracted from bibliographic data.[29] Decreasing values of Wo with temperature were thus obtained from 71,6 mJ/m² for T=295K to 51,8 mJ/m² for T=413K. Although the absolute values of W_0 are subject

to uncertainties related to surface energy estimates, the analysis focuses on relative variations with temperature, which are robust.

Optical profilometry

Optical profilometry images were acquired with a S-Neox from SensoFar® in confocal mode (blue light and objective=X50). Average height profile were extracted using Gwyddion software.

Commenté [DS1]: profiles

Results

In previous works, we have shown that measuring the force needed to detach (i.e. the pull-off force) the AFM tip and a polymer surface[30,31] as function of the temperature allowed the detection of thermomechanical transitions such as bulk Tg or nematic-isotropic transition for polymer films as thin as 7nm.[25,32] It is known that the pull-off force intensity between an AFM tip and a polymer surface is governed, within contact mechanics frameworks, by several factors including: the surface contact area, the surface energies and the elastic properties of both materials.[33,34] In addition, viscoelastic properties of the polymer (i.e. time-dependant adhesion)[35] and environmental factor[36] may have also a consequent influence. By performing, the measurement in controlled media, constant frequency and controlled load force we have shown that our method allows the limitation of the impact of these different factors.[25]

Figure 1 shows the measured pull-off force between an AFM tip and polymer surface as function of the temperature for a PS film (Mn=783k and h=204nm). In previous works,[25,32,37] we have shown that the increase in the pull-off force allows the detection of bulk Tg. It is explained by the observed decrease of the storage modulus at Tg illustrating the transition from the glassy to the rubbery state. Since the polymer film becomes softer, the contact area increases even under the

same load conditions, resulting in an increase in pull-off force. To detect more accurately the Tg we performed a derivative of the pull-off force vs. temperature curve. Tg (i.e. Tg=376K) is detected as the first point of the derivative curve above zero before a strong increase in the derivative. We have confirmed that Tg measured by pull-off force does agree well with those detected by DSC or by ellipsometry measurements (Figure S1).[25] In addition to Tg, a temperature at which the pull-off force reaches a maximum can be detected (i.e. inflexion point of the derivative curve). This temperature will be named T_{max} in the following.

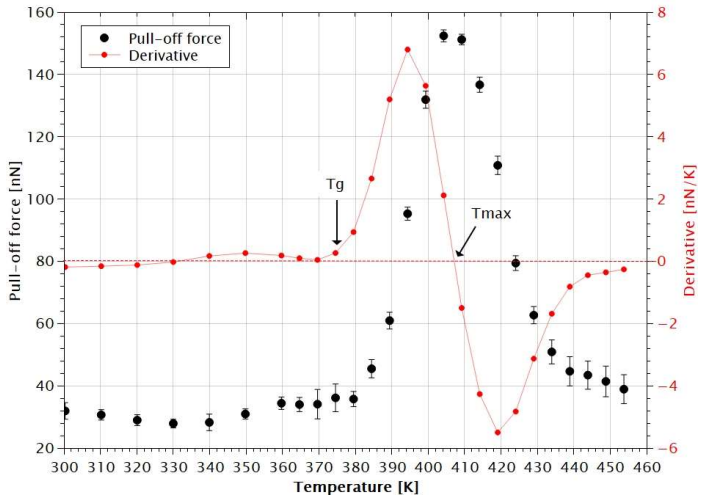

Figure 1. Pull-off force vs. temperature and its derivative curve for a PS supported film (Mn=783k and h=204nm)

The systematic evolution in the shape of the force-distance curves acquired via AFM below and above T_{max}, as illustrated in Figure S3, reveals that, concomitant with a maximum in adhesion force at $T=T_{max}$, a pronounced hysteresis between the approach and retraction curves is observed, alongside a large separation distance defined as the distance between the point of maximum

adhesion and the complete detachment of the AFM tip. These distinctive features are characteristic of a transition from solid/elastic to viscous mechanical behavior.

By performing plotting the pull-off force vs. temperature for different frequencies (i.e. same z range with various approach/retraction duration), a shift in T_{max} towards higher temperatures can be observed (Figure S4). Although the experimentally accessible frequency range is limited, it is demonstrated that the T_{max} shift can be effectively modeled using a Williams, Landel et Ferry equation (WLF). Demonstrating that the WLF is verified allows us to exclude experimental artifacts as the cause of the maximum since WLF implies a cooperative, thermo-activated, free-volume-governed mechanism—exactly what characterizes the dynamics of polymer chains above Tg.[38] The final argument supporting the notion that T_{max} is an intrinsic material property, rather than an optimal measurement condition, is substantiated by the observation of T_{max} across various tested amorphous polymers, irrespective of their chemical composition, molecular weight (Mn), and film thickness (Figure S5).

Although to our best knowledge we are the first team to study that maximum of pull-off force by AFM, it has been already investigated with other techniques.[39–41] Cavities (i.e. pockets of air), present because of initial imperfect contact between the probe and the polymer, can be under tensile stress the seed of two rupture mechanisms. The two failure mechanism can be distinguished by the viscoelastic and surface properties of the polymer surface.[42] On one hand, for high elastic modulus and low tan δ, the rupture by propagation of interfacial cracks will lead to low pull-off force. On the other hand, for low elastic modulus and high tan delta, values growth of the cavities may lead to the formation of complex fibrillar structures that strongly increases the pull-off force.[43,44] The fibrillar structures where observed on several systems including thin polymer films.[45] By measuring the contact area simultaneously with the pull-off force on PMMA surface,

Kim *et al.* confirmed that fibrils were observed at the maximum pull-off force occurring at $T=T_g+40K$.[46] In order to demonstrate that the observed T_{max} in AFM pull-off force measurement is characteristic of the fibrils occurrence, we have studied the viscoelastic properties and pull-off force evolution of a thin PS film (Mn=783k h=104nm).

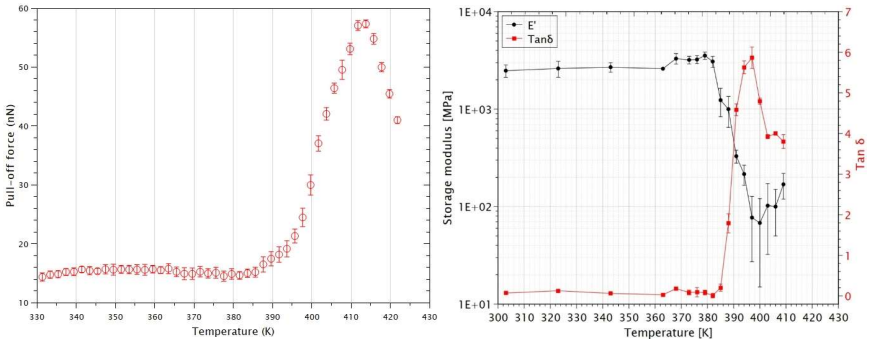

Figure 2. (left) Evolution of the pull-off force and (right) storage modulus (E') and tan δ (f=1Hz) with temperature for a supported PS film (Mn=783k – h=104nm).

Figure 2 shows the measured pull-off forces between an AFM tip and a 140nm thick polystyrene supported film as a function of the temperature and the respective storage modulus E' and tan δ measured by nano-DMA. As discussed before, the increase in pull-off force (Figure 2) from T=Tg=380K may be explained by the observed decrease in the storage modulus (Figure 2) from 3 to 0,1 GPa illustrating the transition from the glassy to the rubbery state. These values agree with those measured by Torres *et al.* for PS thin films.[47] At temperature above Tg+10K, the storage modulus does not vary significantly implying that the observed strong increase in the pull-off force can no longer be explained by a softening of the material. The appropriate parameter to describe a transition between fibrils and crack propagation mechanisms in the case of an elastic rubber has been proposed to be Gc/E'h [48] where Gc is the critical energy release rate and E'h represents the

elastic energy necessary to deform the bulk of a sample of thickness h with elastic modulus E'. In the case of a viscoelastic material, Gc can be approximated by Gc= $W_0 \times \tan \delta$ where W_0 is the work of adhesion between the probe and the polymer.[49] Using the data for E' and tan δ from the nano-DMA experiment and value of W_0 calculated from contact angle measurements (see Experimental part) we were able to plot the parameter space spanned by $W_0 \times \tan \delta$ and $E' \times h$.[42] As shown by Figure 3, two distinct populations can be found: below 385K where Gc/E'h is low and interfacial crack propagation is promoted and above 388K where Gc/Eb is high and bulk rupture mechanism (fibrils) is expected. This result agrees with the study by Nase and demonstrates that at T>385K fibrils start to form in our films. The temperature domain where fibrils can occur is rather narrow. Indeed, at low temperature fibrils cannot form because chains disentanglement is not possible whereas at higher temperature fibrils become instable because the viscosity is too low.[41] This behavior reflects the competition between chain mobility, required for fibril formation, and viscous dissipation, which destabilizes fibrils at high temperature. As a consequence, the pull-off force should decrease. This result indicates that T_{max} may be seen as the temperature where fibrils are the strongest. T_{max} can thus be defined as the temperature at which cohesive fibrillation during debonding of the polymer layer is mechanically optimal, corresponding to a balance between chain mobility and viscous dissipation, and leading to a maximum resistance to separation.

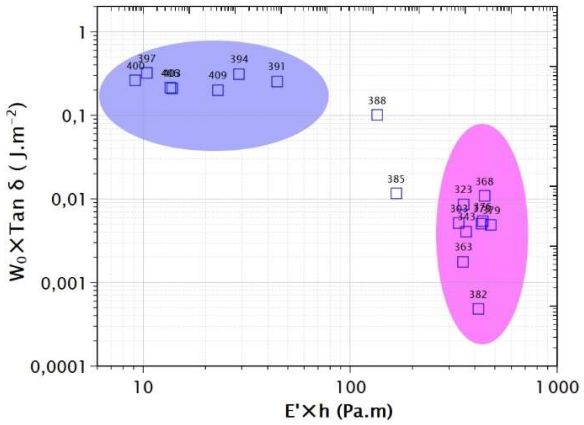

Figure 3. Map of the top region corresponds to temperatures where bulk rupture mechanism is expected. Low region corresponds to temperatures where interfacial crack propagation is promoted.

Effect of Mn

To investigate how the polymer chain length may influence the value of Tmax we have studied the pull-off force vs temperature of PS supported films with different Mn (Figure 4). In order to prevent any confinement effect which will be studied later we chose to study polymer films with thickness above 100nm.

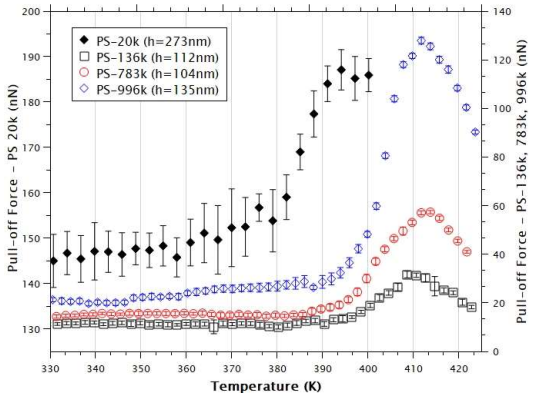

Figure 4. Pull-off force vs. temperature for PS supported film with thicknesses above 100 nm and different Mn.

Even if the absolute pull-off force may differ from one AFM tip to another it can be seen in Table 1 that the relative pull-off force at Tmax (i.e. pull-off force at Tmax normalized by pull-off force at 293K) increases with Mn. These results agree with those of Zosel *et al.* for monodisperse Polybutadiene[50] and it can be explained by an increase in viscosity when Mn increases leading to an increase in cohesive strength and a higher stability of the fibrils. For Mn>136k, the values of Tg bulk and Tmax remain unchanged. For low Mn, (Mn=20k) a shift of both Tg and Tmax toward the low temperature values is observed. Whereas the decrease in Tg is expected for Mn=20k[51] the fact that Tmax decreases also seems to indicate that for PS, Tmax is also probably related to chain dynamics which governs the glass transition mechanism. The link between Tg and Tmax is highlighted by the value of the Tmax/Tg which remains constant independently on the Mn (Table 1).

Table 1. Measured and calculated quantities extracted from Figure 4 with their uncertainties.

	Tg (K)	Tmax (K)	Tmax/Tg	Relative pull-off force at Tmax
20k	358(3)	395(2)	1.10 (0.01)	1.29
136k	380(3)	410(2)	1.08 (0.01)	2.43
783k	382(2)	413(2)	1.08 (0.01)	3.90
996k	379(2)	412(2)	1.09 (0.01)	5.67

Recent work on glass transition has demonstrated that for polymer glass to become liquid, it is not sufficient to simply overcome the interparticle binding energies. Instead, more energy must be invested to break up the typical cooperative particle network that is common to glassy materials.[52] In addition, Peng *et al.* investigated PS chain dynamics at temperatures above Tg by ^{1}H NMR.[8] They found two transition temperatures T_f=1.1×Tg that can be associated with the melting process of polymeric rigid components and Tc=1.2×Tg where the complete disappearance of the rigid components occurs and that the polystyrene became a homogenous isotropic liquid. This last temperature (Tc) is similar to the predicted critical temperature (1.2×Tg) by mode coupling theory and liquid-liquid transition prediction.[16,53] ~~We can thus assume that Tmax is probably the Tf measured by Peng *et al.* within the experimental resolution of the present method and corresponds to the beginning of the transition between a rubber and a liquid phase which end at the crossover~~

~~temperature (Tc).~~Interestingly, by studying the pull off force at higher temperature, as shown on Figure 1, it can be seen that after T_{max}, the pull-off force value decreases until it reaches a stable value when T=455K =1,2×Tg. Since for a liquid it is known that the surface adhesion is mainly governed by interfacial surface energy rather than mechanical properties, the pull-off force variation is weak. These findings tend to indicate that the polymer film behaves like an isotropic liquid above T= 1,2Tg. Two additional experimental findings support the hypothesis that T_{max} may correspond to the onset of a rubber-liquid transition. The first of these findings is detailed below, involving the examination of the morphological evolution of a scratch on a PS-783k (h=0.9µm) film as a function of temperature, utilizing optical profilometry (Figure 5). Initially (T=303K) the scratch width and height extracted from a negative step height function fitting are 26,0 µm and 0.9 µm respectively. After 1min at T=Tg=383K no significant modification of the morphology can be seen. After 1min at T=Tmax=413K the width of the scratch decreases to 18,1 µm demonstrating the recovery of the scratch (70%) due to a drastic decrease of viscosity of the polymer at this temperature.[54]

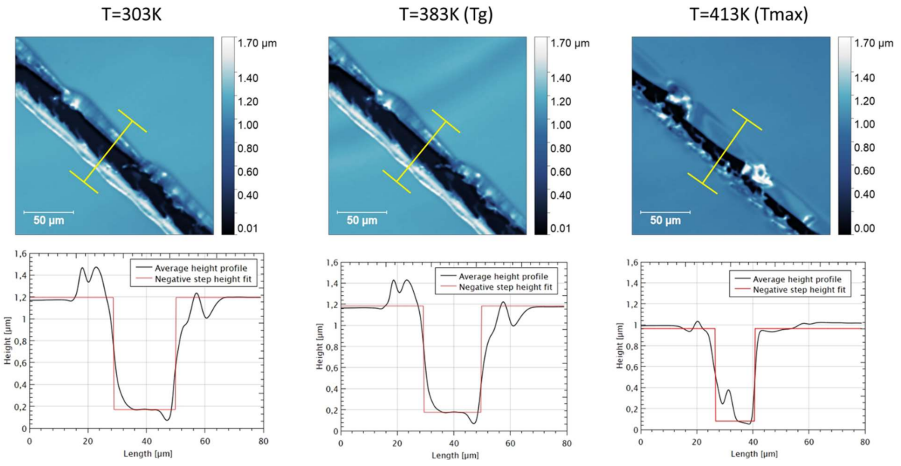

Figure 5. Optical profilometry image of a scratch made on a supported PS-783k (h=0.9µm) film as function of the substrate temperature and corresponding average profiles and fits showing

The second finding that supports a significant alteration in chain dynamics at Tmax, leading to polymer flow, is derived from our previous research on synthesized amorphous azobenzene polymers exhibiting liquid-crystal properties. Our study demonstrated that at T=Tmax, a transition from solid to liquid was observed, and Tmax corresponds to the nematic-isotropic transition temperature, where the liquid crystal structure is lost.[32]

All these experimental results tend to show that T_{max} may be seen as the beginning of a rubber to liquid phase transition temperature of the polymer film. However, due to the inability to establish time-temperature scaling in this study, the hypothesis that this transition concludes at the crossover temperature (Tc) remains unconfirmed.

Confinement effect

Numerous previous studies have shown that reducing film thickness below 100 nm can lead for PS supported film on SiOx substrate to a decrease in the measured Tg until film thickness is below ~10 nm where Tg values remained constant, around 355 K.[55–57] Since, for this system, it is accepted that after annealing the substrate/PS interactions are weak and do not influence the chain dynamics,[58,59] the origin of this decrease is the presence of a surface mobile layer where the chain mobility is enhanced and lead to a “surface Tg” close to 350-360 K.

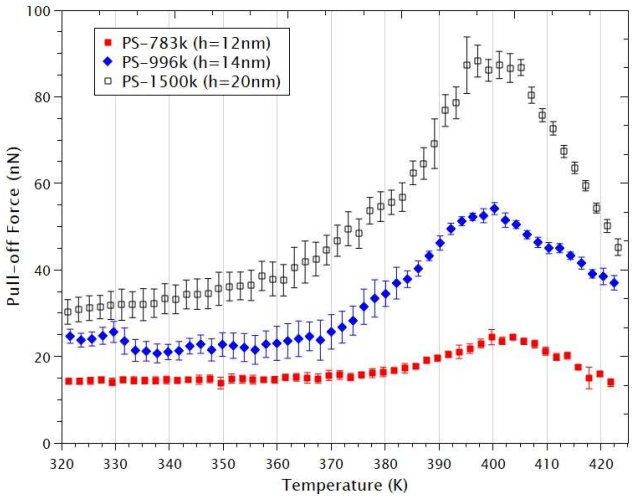

Figure 6. Pull-off force vs. temperature curves for thin film (h<20nm) of different Mn

Table 2. Measured Tg, Tmax and Tmax/Tg ratio extracted from Figure 6

	Tg [K]	Tmax [K]	Tmax/Tg
783k	356(2)	401(2)	1.13(0.01)
996k	354(2)	400(2)	1.13(0.01)
1500k	351(2)	400(2)	1.14(0.01)

Figure 6 shows the pull-off force vs. temperature curves obtained for different PS films with different Mn and thicknesses below 20 nm. Compared to thicker film (Table 1), all the films show a decrease in Tg (15 to 20K) characteristic of the confinement effect (Table 2). The independence of the Tg depression with Mn agrees with previous work.[52] T_{max} value also decreases compared to thicker films and an increase in the T_{max}/Tg ratio up to 1.13 is observed. Several theoretical works have linked the value of Tc/Tg to the fragility of the glass former. Polymer fragility (m) quantifies the rate at which relaxation time (or viscosity) rises as temperature decreases toward Tg, compared to an ideal Arrhenius behaviour. In polymers, the ratio Tc/Tg is known to grow when m decrease.[5] Since the fragility of PS is known to decrease with film thickness,[60] the observed elevation in the T_{max}/Tg_ratio under conditions of confinement appears to corroborate the hypothesis that T_{max} may be intrinsically related to Tc. Nevertheless, comprehensive time- and temperature-dependent investigations are warranted to substantiate this putative correspondence. ~~the observed increase in the T_{max}/Tg ratio with confinement is consistent with the hypothesis that T_{max} is closely related to Tc and confirm our hypothesis that Tmax is the beginning of the rubber to liquid transition which end at the crossover temperature (Tc).~~

Conclusion

By performing AFM pull-off force measurements as a function of temperature, the presence of a temperature at which the pull-off force is maximum (T_{max}) has been demonstrated over a wide range of amorphous polymers. Nano-DMA measurements have demonstrated the link between T_{max} and the fibril formation during the adhesion process and the polymer viscosity. Overall, T_{max} corresponds to a mechanical optimum of cohesive fibrillation during debonding, arising from a balance between chain mobility and viscous dissipation. Measurements performed on supported monodisperse PS films with controlled thicknesses demonstrated that regardless of the film

thickness (i.e., with or without confinement effect), the T_{max}/Tg ratio is independent of Mn. However, this ratio rises when the films are confined. To interpret these results, we propose that T_{max} can be seen as the onset temperature of the rubber-liquid transition~~., which ends at the crossover temperature (Tc) predicted by the MCT theory~~. Even if further work is required to support such claims, the influence of polymer fragility on this transition appears to play a significant role. The possible relation between T_{max} and the crossover temperature (Tc) predicted by the MCT theory deserve to be investigated. To the best of our knowledge, this is the first study to investigate the effect of confinement on the rubber-to-liquid transition in polymer films. Further studies are needed to accurately characterize the position of this characteristic temperature and its dependence on polymer properties (chemistry, dispersity, etc.) or to elucidate its molecular origin. The methodology developed in the present study constitutes a novel experimental approach for investigating the rubber-to-liquid transition in polymers, with significant potential applications across diverse fields of polymer science. In the domain of polymer adhesives, adhesion properties are optimized at this characteristic temperature, while the approach also holds relevance in polymer processing.

ACKNOLEDGMENTS

We gratefully thank Pierre Nickmilder for his help with the acquisition of the nanoDMA data.

REFERENCES

(1) Novikov, V. N.; Sokolov, A. P. Temperature Dependence of Structural Relaxation in Glass-Forming Liquids and Polymers. *Entropy* **2022**, *24* (8), 1101.

(2) Baker, D. L.; Reynolds, M.; Masurel, R.; Olmsted, P. D.; Mattsson, J. Cooperative Intramolecular Dynamics Control the Chain-Length-Dependent Glass Transition in Polymers. *Phys. Rev. X* **2022**, *12* (2), 021047. https://doi.org/10.1103/PhysRevX.12.021047.

(3) Ferry, J. D.; Fitzgerald, E. R.; Grand, L. D.; Williams, M. L. Temperature Dependence of Dynamic Mechanical Properties of Elastomers, Relaxation Distributions. *Ind. Eng. Chem.* **1952**, *44* (4), 703–706. https://doi.org/10.1021/ie50508a018.

(4) Dudognon, E.; Bernès, A.; Lacabanne, C. Low-Frequency Chain Dynamics of Poly(n-Hexyl Methacrylate) by Dielectric Spectroscopies. *Macromolecules* **2002**, *35* (15), 5927–5931. https://doi.org/10.1021/ma012243x.

(5) Pawlus, S.; Kunal, K.; Hong, L.; Sokolov, A. P. Influence of Molecular Weight on Dynamic Crossover Temperature in Linear Polymers. *Polymer* **2008**, *49* (12), 2918–2923. https://doi.org/10.1016/j.polymer.2008.04.040.

(6) Shang, S.; Wu, X.; Zhu, Z. Energy Dissipation Study of Atactic Polystyrene Melts above *T*g. *Phys. B Condens. Matter* **2007**, *396* (1), 160–163. https://doi.org/10.1016/j.physb.2007.03.030.

(7) X. B. Wu; S. Y. Shang; Q. L. Xu; Z. G. Zhu. Effects of Molecular Weight on the Liquid-Liquid Transition in Polystyrene Melts Studied by Low-Frequency Anelastic Spectroscopy. *J. Appl. Phys.* **2008**, *103* (7), 073519. https://doi.org/10.1063/1.2904588.

(8) Peng, Y.; Cai, C.; Zhang, R.; Chen, T.; Sun, P.; Li, B.; Wang, X.; Xue, G.; Shi, A.-C. Probing the Two-Stage Transition upon Crossing the Glass Transition of Polystyrene by Solid-State NMR. *Chin. J. Polym. Sci.* **2016**, *34* (4), 446–456. https://doi.org/10.1007/s10118-016-1762-z.

(9) Boyer, R. F. The Relation of Transition Temperatures to Chemical Structure in High Polymers. *Rubber Chem. Technol.* **1963**, *36* (5), 1303–1421. https://doi.org/10.5254/1.3539649.

(10) Boyer, R. F. Evidence from T Ll and Related Phenomena for Local Structure in the Amorphous State of Polymers. In *Order in the Amorphous "State" of Polymers*; Keinath, S. E., Miller, R. L., Rieke, J. K., Eds.; Springer US: Boston, MA, 1987; pp 135–185.

(11) Glandt, C. A.; Toh, H. K.; Gillham, J. K.; Boyer, R. F. Effect of Dispersity on the Tll (>Tg) Transition in Polystyrene. *J. Appl. Polym. Sci.* **1976**, *20* (5), 1277–1288. https://doi.org/10.1002/app.1976.070200511.

(12) Orbon, S. J.; Plazek, D. J. Some Evidence against the Existence of the Liquid-Liquid Transition. IV. The Temperature Dependence of Shear Viscosity. *J. Polym. Sci. Polym. Phys. Ed.* **1982**, *20* (9), 1575–1583. https://doi.org/10.1002/pol.1982.180200906.

(13) Ibar, J. P. A Dual-Phase Approach to Reveal the Presence and Impact of the TLL Transition in Polymer Melts. Part II. The Theoretical and Practical Relevance of the TLL Existence and Characteristics on the Understanding of the Melt Thermal Analysis and Rheological Properties of Polymers: Duality and Cross-Duality of the Interactions. *J. Macromol. Sci. Part B* **2021**, *60* (10), 792–838. https://doi.org/10.1080/00222348.2021.1913370.

(14) Hedvat, S. Molecular Interpretation of T‖, the Rubbery-Viscous 'Transition' Temperature of Amorphous Polymers. *Polymer* **1981**, *22* (6), 774–777. https://doi.org/10.1016/0032-3861(81)90013-6.

(15) Janssen, L. M. C. Mode-Coupling Theory of the Glass Transition: A Primer. *Front. Phys.* **2018**, *6*. https://doi.org/10.3389/fphy.2018.00097.

(16) Kisliuk, A.; Mathers, R. T.; Sokolov, A. P. Crossover in Dynamics of Polymeric Liquids: Back to Tll? *J. Polym. Sci. Part B Polym. Phys.* **2000**, *38* (21), 2785–2790. https://doi.org/10.1002/1099-0488(20001101)38:21<2785::AID-POLB70>3.0.CO;2-S.

(17) W. Gotze; L. Sjogren. Relaxation Processes in Supercooled Liquids. *Rep. Prog. Phys.* **1992**, *55* (3), 241. https://doi.org/10.1088/0034-4885/55/3/001.

(18) Pihlajamaa, I.; Debets, V. E.; Laudicina, C. C. L.; Janssen, L. M. C. Unveiling the Anatomy of Mode-Coupling Theory. *SciPost Phys.* **2023**, *15* (5). https://doi.org/10.21468/SCIPOSTPHYS.15.5.217.

(19) Luo, C.; Janssen, L. M. C. Generalized Mode-Coupling Theory of the Glass Transition. II. Analytical Scaling Laws. *J. Chem. Phys.* **2020**, *153* (21), 214506. https://doi.org/10.1063/5.0026979.

(20) Tian, H.; Xu, Q.; Zhang, H.; Priestley, R. D.; Zuo, B. Surface Dynamics of Glasses. *Appl. Phys. Rev.* **2022**, *9* (1), 011316. https://doi.org/10.1063/5.0083726.

(21) Li, B.; Zhang, S.; Andre, J. S.; Chen, Z. Relaxation Behavior of Polymer Thin Films: Effects of Free Surface, Buried Interface, and Geometrical Confinement. *Prog. Polym. Sci.* **2021**, *120*, 101431. https://doi.org/10.1016/j.progpolymsci.2021.101431.

(22) Napolitano, S.; Glynos, E.; Tito, N. B. Glass Transition of Polymers in Bulk, Confined Geometries, and near Interfaces. *Rep Prog Phys* **2017**, *80*, 036602.

(23) Bal, J. K.; Beuvier, T.; Unni, A. B.; Chavez Panduro, E. A.; Vignaud, G.; Delorme, N.; Chebil, M. S.; Grohens, Y.; Gibaud, A. Stability of Polymer Ultrathin Films (<7 Nm) Made by a Top-Down Approach. *ACS Nano* **2015**, *9* (8), 8184–8193. https://doi.org/10.1021/acsnano.5b02381.

(24) Unni, A. B.; Vignaud, G.; Chapel, J. P.; Giermanska, J.; Bal, J. K.; Delorme, N.; Beuvier, T.; Thomas, S.; Grohens, Y.; Gibaud, A. Probing the Density Variation of Confined Polymer Thin Films via Simple Model-Independent Nanoparticle Adsorption. *Macromolecules* **2017**, *50* (3), 1027–1036. https://doi.org/10.1021/acs.macromol.6b02617.

(25) Delorme, N.; Chebil, M. S.; Vignaud, G.; Le Houerou, V.; Bardeau, J. F.; Busselez, R.; Gibaud, A.; Grohens, Y. Experimental Evidence of Ultrathin Polymer Film Stratification by AFM Force Spectroscopy. *Eur Phys J E* **2015**, *38*, 56. https://doi.org/10.1140/epje/i2015-15056-9.

(26) Vignaud, G.; Bardeau, J. F.; Gibaud, A.; Grohens, Y. Multiple Glass-Transition Temperatures in Thin Supported Films of Isotactic PMMA as Revealed by Enhanced Raman Scattering. *Langmuir* **2005**, *21* (19), 8601–8604. https://doi.org/10.1021/la050898b.

(27) Pittenger, B.; Osechinskiy, S.; Yablon, D.; Mueller, T. Nanoscale DMA with the Atomic Force Microscope: A New Method for Measuring Viscoelastic Properties of Nanostructured Polymer Materials. *JOM* **2019**, *71* (10), 3390–3398. https://doi.org/10.1007/s11837-019-03698-z.

(28) Georgiev, G. A.; Baluschev, S.; Eftimov, P.; Bacheva, M.; Landfester, K. Addressing the Apparent Controversies Between the Contact Angle-Based Models for Estimation of Surface Free Energy: A Critical Review. *Colloids Interfaces* **2024**, *8* (6), 62. https://doi.org/10.3390/colloids8060062.

(29) Wang, J.; Zhang, K.; Wang, F.; Zheng, W. Improving Frictional Properties of DLC Films by Surface Energy Manipulation. *RSC Adv.* **2018**, *8* (21), 11388–11394. https://doi.org/10.1039/C8RA00580J.

(30) Bliznyuk, V. N.; Assender, H. E.; Briggs, G. A. D. Surface Glass Transition Temperature of Amorphous Polymers. A New Insight with SFM. *Macromolecules* **2002**, *35* (17), 6613–6622. https://doi.org/10.1021/ma011326a.

(31) Tsui, O. K. C.; Wang, X. P.; Ho, J. Y. L.; Ng, T. K.; Xiao, X. Studying Surface Glass-to-Rubber Transition Using Atomic Force Microscopic Adhesion Measurements. *Macromolecules* **2000**, *33* (11), 4198–4204. https://doi.org/10.1021/ma991473x.

(32) Siniscalco, D.; Pessoni, L.; Billon, L.; Boussonnière, A.; Castanet, A.-S.; Bardeau, J.-F.; Nickmilder, P.; Leclère, P.; Delorme, N. Measurement of the Transition Temperature Governing the Photoinduced Reversible Solid-to-Liquid Transition of Azobenzene-Containing Polymers. *ACS Appl. Polym. Mater.* **2023**, *5* (9), 7358–7363. https://doi.org/10.1021/acsapm.3c01256.

(33) Derjaguin, B. V.; Muller, V. M.; Toporov, Y. P. Effect of Contact Deformations on the Adhesion of Particles. *J. Colloid Interface Sci.* **1975**, *53* (2), 314–326. https://doi.org/10.1016/0021-9797(75)90018-1.

(34) Johnson, K. L.; Kendall, K.; Roberts, A. D. Surface Energy and the Contact of Elastic Solids. *Proc. R. Soc. Lond. Math. Phys. Sci.* **1971**, *324* (1558), 301–313. https://doi.org/doi:10.1098/rspa.1971.0141.

(35) Onozuka, N.; Nakajima, K. Atomic Force Microscopy Analysis of Velocity Dependent Adhesive Viscoelastic Contact. *Langmuir* **2024**, *40* (46), 24565–24575. https://doi.org/10.1021/acs.langmuir.4c03370.

(36) Butt, H.-J.; Barnes, W. J. P.; del Campo, A.; Kappl, M.; Schonfeld, F. Capillary Forces between Soft, Elastic Spheres. *Soft Matter* **2010**, *6* (23), 5930–5936. https://doi.org/10.1039/c0sm00455c.

(37) Pessoni, L.; Siniscalco, D.; Boussonnière, A.; Castanet, A.-S.; Billon, L.; Delorme, N. Photo-Reversible Solid to Liquid Transition of Azobenzene Containing Polymers: Impact of the Chemical Structure and Chain Length. *Eur. Polym. J.* **2022**, *174*, 111297. https://doi.org/10.1016/j.eurpolymj.2022.111297.

(38) Landel, R. F. The Temperature Dependence of Viscoelastic Responses above Tg. *J. Acoust. Soc. Am.* **2005**, *82* (S1), S85. https://doi.org/10.1121/1.2025030.

(39) Creton, C.; Fabre, P. Tack. In *The Mechanics of Adhesion*; 2002; Vol. 2, pp 535–575.

(40) Gay, C.; Leibler, L. Theory of Tackiness. *Phys. Rev. Lett.* **1999**, *82* (5), 936–939. https://doi.org/10.1103/PhysRevLett.82.936.

(41) Lakrout, H.; Sergot, P.; Creton, C. Direct Observation of Cavitation and Fibrillation in a Probe Tack Experiment on Model Acrylic Pressure-Sensitive-Adhesives. *J. Adhes.* **1999**, *69* (3–4), 307–359. https://doi.org/10.1080/00218469908017233.

(42) Nase, J.; Lindner, A.; Creton, C. Pattern Formation during Deformation of a Confined Viscoelastic Layer: From a Viscous Liquid to a Soft Elastic Solid. *Phys. Rev. Lett.* **2008**, *101* (7), 074503. https://doi.org/10.1103/PhysRevLett.101.074503.

(43) Zosel, A. The Effect of Fibrilation on the Tack of Pressure Sensitive Adhesives. *Int. J. Adhes. Adhes.* **1998**, *18* (4), 265–271. https://doi.org/10.1016/S0143-7496(98)80060-2.

(44) Zosel, A. Adhesion and Tack of Polymers: Influence of Mechanical Properties and Surface Tensions. *Colloid Polym. Sci.* **1985**, *263* (7), 541–553. https://doi.org/10.1007/BF01421887.

(45) Zeng, H.; Zhao, B.; Israelachvili, J. N.; Tirrell, M. Liquid- to Solid-Like Failure Mechanism of Thin Polymer Films at Micro- and Nanoscales. *Macromolecules* **2010**, *43* (1), 538–542. https://doi.org/10.1021/ma901845z.

(46) Kim, K.-S.; Heo, J.-C.; Kim, K.-W. Effects of Temperature on the Microscale Adhesion Behavior of Thermoplastic Polymer Film. *Tribol. Lett.* **2010**, *38* (2), 97–106. https://doi.org/10.1007/s11249-010-9578-4.

(47) Torres, J. M.; Stafford, C. M.; Vogt, B. D. Impact of Molecular Mass on the Elastic Modulus of Thin Polystyrene Films. *Polymer* **2010**, *51* (18), 4211–4217. https://doi.org/10.1016/j.polymer.2010.07.003.

(48) Webber, R. E.; Shull, K. R.; Roos, A.; Creton, C. Effects of Geometric Confinement on the Adhesive Debonding of Soft Elastic Solids. *Phys. Rev. E* **2003**, *68* (2), 021805. https://doi.org/10.1103/PhysRevE.68.021805.

(49) Maugis, D.; Barquins, M. Fracture Mechanics and the Adherence of Viscoelastic Bodies. *J. Phys. Appl. Phys.* **1978**, *11* (14), 1989. https://doi.org/10.1088/0022-3727/11/14/011.

(50) ZOSEL, A. Fracture Energy and Tack of Pressure Sensitive Adhesives. *Adv. Press. Sensitive Adhes. Technol.* **1992**, *1*, 92–127.

(51) Fox, T. G.; Loshaek, S. Influence of Molecular Weight and Degree of Crosslinking on the Specific Volume and Glass Temperature of Polymers. *J. Polym. Sci.* **1955**, *15* (80), 371–390. https://doi.org/10.1002/pol.1955.120158006.

(52) Lunkenheimer, P.; Loidl, A.; Riechers, B.; Zaccone, A.; Samwer, K. Thermal Expansion and the Glass Transition. *Nat. Phys.* **2023**, *19* (5), 694–699. https://doi.org/10.1038/s41567-022-01920-5.

(53) Boyer, R. F. Pressure Dependence of Secondary Transitions in Amorphous Polymers. 1. Tll for Polystyrene, Poly(Vinyl Acetate), and Polyisobutylene. *Macromolecules* **1981**, *14* (2), 376–385. https://doi.org/10.1021/ma50003a028.

(54) Willocq, B.; Khelifa, F.; Odent, J.; Lemaur, V.; Yang, Y.; Leclère, P.; Cornil, J.; Dubois, P.; Urban, M. W.; Raquez, J.-M. Mechanistic Insights on Spontaneous Moisture-Driven Healing of Urea-Based Polyurethanes. *ACS Appl. Mater. Interfaces* **2019**, *11* (49), 46176–46182. https://doi.org/10.1021/acsami.9b16858.

(55) Ma, Z.; Nie, H.; Tsui, O. K. C. Substrate Influence on the Surface Glass Transition Temperature of Polymers. *Polymer* **2024**, *312*, 127594. https://doi.org/10.1016/j.polymer.2024.127594.

(56) Kim, S.; Hewlett, S. A.; Roth, C. B.; Torkelson, J. M. Confinement Effects on Glass Transition Temperature, Transition Breadth, and Expansivity: Comparison of Ellipsometry and Fluorescence Measurements on Polystyrene Films. *Eur. Phys. J. E* **2009**, *30* (1), 83–92. https://doi.org/10.1140/epje/i2009-10510-y.

(57) Keddie, J. L.; Jones, R. A. L.; Cory, R. A. Size-Dependent Depression of the Glass Transition Temperature in Polymer Films. *Eur. Lett* **1994**, *27*, 59.

(58) Kanaya, T.; Miyazaki, T.; Watanabe, H.; Nishida, K.; Yamano, H.; Tasaki, S.; Bucknall, D. B. Annealing Effects on Thickness of Polystyrene Thin Films as Studied by Neutron Reflectivity. *Polymer* **2003**, *44* (14), 3769–3773. http://dx.doi.org/10.1016/S0032-3861(03)00309-4.

(59) Yan, J.; Ma, Z.; Xu, J.; Nie, H.; Yuan, H.; Wang, X.; Wang, T.; Weng, L.-T.; Tsui, O. K. C. Glass Transition of the Surface Monolayer of Polystyrene Films: Effect of Thermal Preannealing. *Macromolecules* **2023**, *56* (15), 5917–5923. https://doi.org/10.1021/acs.macromol.3c00966.

(60) Lan, T.; Torkelson, J. M. Fragility-Confinement Effects: Apparent Universality as a Function of Scaled Thickness in Films of Freely Deposited, Linear Polymer and Its Absence in Densely Grafted Brushes. *Macromolecules* **2016**, *49* (4), 1331–1343. https://doi.org/10.1021/acs.macromol.5b02489.

ASSOCIATED CONTENT

Figure S1

Glass temperature transitions (Tg) measured by DSC of the PS samples used in this work

Mn (g/mol)	20k	136k	783k	996k	1500k
Tg by DSC	361(2)	377(2)	378(2)	376(2)	378(2)

Figure S2

Influence of AFM tip geometry, chemical nature and stiffness on the detection of T_{max} for a PS-783k (h=114nm) film.

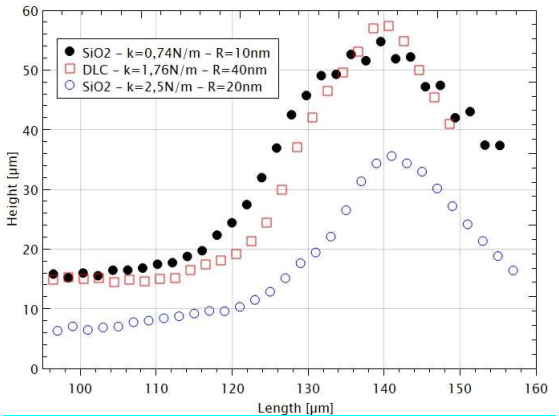

Figure S3

Evolution of the approach-retracting force distance curves with temperature.

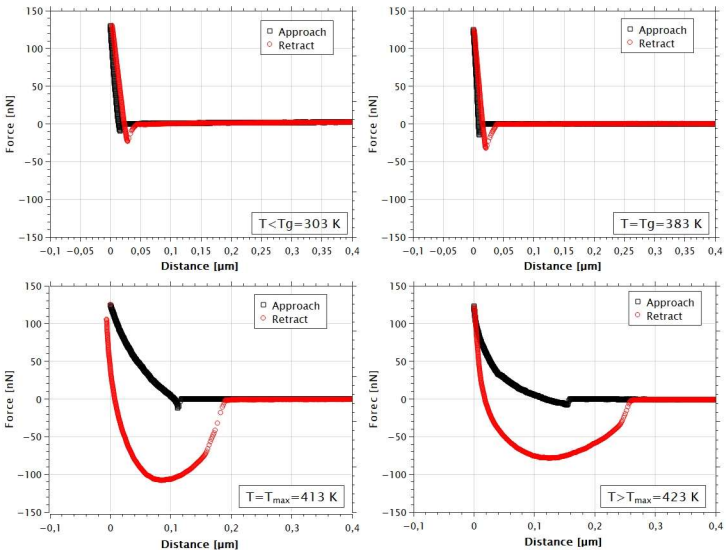

Figure S4

Evolution with approach-retraction frequency of the pull-off force vs temperatures curves for a PS-783k (h=108nm) and corresponding WLF curve fitting of the measured T_{max}

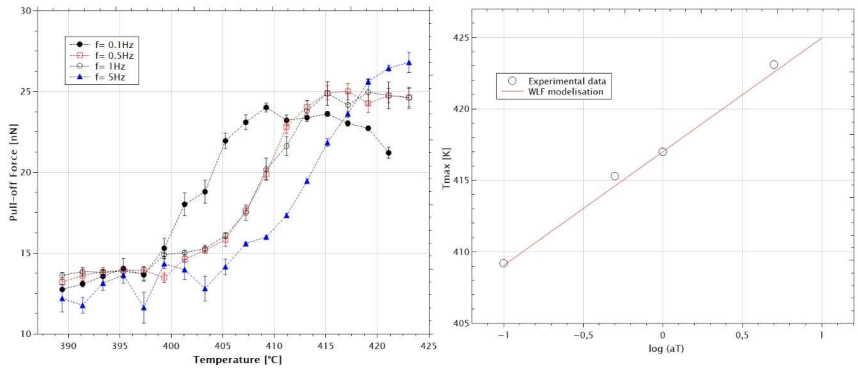

Figure S5

Pull-off force vs. temperature for PS, iPMMA and PBMA films supported on SiOx with different Mn and film thicknesses. Dash and full vertical lines indicate bulk Tg and Tmax respectively